Angiogenesis (2019) 22:37–52
https://doi.org/10.1007/s10456-018-9635-4

ORIGINAL PAPER

Cellular self-assembly into 3D microtissues enhances the angiogenic activity and functional neovascularization capacity of human cardiopoietic stem cells

Petra Wolint[1] · Annina Bopp[1,2] · Anna Woloszyk[1,2] · Yinghua Tian[1,3] · Olivera Evrova[1,4,5] · Monika Hilbe[6] · Pietro Giovanoli[1,5] · Maurizio Calcagni[1,5] · Simon P. Hoerstrup[2,7] · Johanna Buschmann[1,5] · Maximilian Y. Emmert[2,7,8]

Received: 12 January 2018 / Accepted: 3 July 2018 / Published online: 16 July 2018

Abstract

While cell therapy has been proposed as next-generation therapy to treat the diseased heart, current strategies display only limited clinical efficacy. Besides the ongoing quest for the ideal cell type, in particular the very low retention rate of single-cell (SC) suspensions after delivery remains a major problem. To improve cellular retention, cellular self-assembly into 3D microtissues (MTs) prior to transplantation has emerged as an encouraging alternative. Importantly, 3D-MTs have also been reported to enhance the angiogenic activity and neovascularization potential of stem cells. Therefore, here using the chorioallantoic membrane (CAM) assay we comprehensively evaluate the impact of cell format (SCs versus 3D-MTs) on the angiogenic potential of human cardiopoietic stem cells, a promising second-generation cell type for cardiac repair. Biodegradable collagen scaffolds were seeded with human cardiopoietic stem cells, either as SCs or as 3D-MTs generated by using a modified hanging drop method. Thereafter, seeded scaffolds were placed on the CAM of living chicken embryos and analyzed for their perfusion capacity in vivo using magnetic resonance imaging assessment which was then linked to a longitudinal histomorphometric ex vivo analysis comprising blood vessel density and characteristics such as shape and size. Cellular self-assembly into 3D-MTs led to a significant increase of vessel density mainly driven by a higher number of neo-capillary formation. In contrast, SC-seeded scaffolds displayed a higher frequency of larger neo-vessels resulting in an overall 1.76-fold higher total vessel area (TVA). Importantly, despite that larger TVA in SC-seeded group, the mean perfusion capacity (MPC) was comparable between groups, therefore suggesting functional superiority together with an enhanced perfusion efficacy of the neo-vessels in 3D-MT-seeded scaffolds. This was further underlined by a 1.64-fold higher *perfusion ratio* when relating MPC to TVA. Our study shows that cellular self-assembly of human cardiopoietic stem cells into 3D-MTs substantially enhances their overall angiogenic potential and their functional neovascularization capacity. Hence, the concept of 3D-MTs may be considered to increase the therapeutic efficacy of future cell therapy concepts.

Keywords Cardiopoietic stem cells · Angiogenesis · Neovascularization · Perfusion capacity · Chorioallantoic membrane (CAM) assay · Microtissues · Three dimensional

Abbreviations

2D	Two-dimensional
3D	Three-dimensional
3D-MT	Three-dimensional microtissue
AMI	Acute myocardial infarction
A_R	Aspect ratio
BM	Bone marrow
CAM	Chorioallantoic membrane
CHF	Chronic heart failure
ECM	Extracellular matrix
H&E	Haematoxylin and eosin
hPL	Human platelet lysate
ID	Incubation day

Petra Wolint and Annina Bopp have contributed equally to this study (shared first authorship).

Johanna Buschmann and Maximilian Y. Emmert have contributed equally to this study (shared last authorship).

✉ Simon P. Hoerstrup
simon.hoerstrup@irem.uzh.ch

✉ Maximilian Y. Emmert
maximilian.emmert@usz.ch

Extended author information available on the last page of the article

LV	Left ventricular
MPC	Mean perfusion capacity
MRI	Magnetic resonance imaging
MSCs	Mesenchymal stem cells
ROIs	Regions of interest
SC	Single cell
SD	Standard deviations
SEM	Scanning electron microscope
VEGF	Vascular endothelial growth factor
TVA	Total vessel area

Introduction

Regenerative medicine has been suggested as next-generation strategy to address acute and chronic degenerative diseases affecting different organ systems [1–3]. In particular, the repair and regeneration of the diseased heart has gained substantial popularity. In case of acute myocardial infarction (AMI) or chronic heart failure (CHF), most of the currently available treatment options (i.e., medication, percutaneous interventions, or surgery) are only symptomatic, but do not cure the disease [4]. Therefore, the concept of cell therapy has created substantial hope for the treatment of the diseased heart. To date, numerous stem cell types are under clinical evaluation for their cardioreparative and regenerative potential [5]. However, despite all enthusiasm, for the majority of cell types current clinical data only display limited efficacy to improve cardiac performance after AMI or CHF [6–8]. Notably, most of the clinical trials have utilized unselected, the so-called first-generation cell types, while more recent studies have utilized the so-called second-generation cell types, which are supposed to harbor a higher cardioreparative capacity [5].

As one encouraging example, the concept of mesenchymal stem cell (MSC) lineage specification through guided cardiopoiesis has been recently introduced [9, 10]. Based on promising data from a murine CHF model [11], such human cardiopoietic MSCs have been advanced into a clinical pilot study (C-CURE trial; NCT00810238) [12] and are currently being evaluated for their efficacy in large-scale, multicenter trials (CHART program: CHART-1 trial; NCT01768702, and CHART-2 trial; NCT02317458) [13, 14]. In addition, in a recent translational large animal study, we demonstrated the safety and efficacy of human cardiopoietic stem cells after transcatheter intramyocardial transplantation into porcine hearts with post-infarction left ventricular (LV) dysfunction [15]. At follow-up, cardiopoietic cell-treated animals exhibited a higher ejection fraction and a reduced infarct size when compared to controls. Post-mortem analysis 30 days post transplantation suggested that the beneficial effects were primarily driven by paracrine mechanisms such as neoangiogenesis, but not via (trans-) differentiation into new cardiomyocytes.

Besides the quest for the ideal cell type, appropriate cellular retention after delivery seems to play a key role in order to achieve and enhance therapeutic efficacy. In this regard, recent data indicate that cellular retention and integration significantly depends on the format the cells are applied to the heart. Although they are easy to deliver to the myocardium via a catheter-based approach, various reports have highlighted that the cellular retention after single-cell (SC) injections is rather low as most of the injected cells are lost to the circulation [16]. In order to improve that, several three-dimensional (3D) cell and micro-scale tissue engineering concepts have been proposed [17]. However, most of such concepts are scaffold-based [18], and hence primarily require surgical approaches for their delivery thereby increasing procedural complexity and invasiveness [19]. Hence, a scaffold-free 3D cell format would represent the ideal approach in order to achieve both, an enhanced cellular retention along with the feasibility of a catheter-based, minimally invasive delivery technique.

As one example, the use of scaffold-free 3D cell aggregates or the so-called microtissues (3D-MTs) has been suggested as an interesting strategy to accomplish these goals [20]. Various fabrication methods for 3D-MTs have been developed and tested [21–24] demonstrating their superiority of 3D-MTs over SC cultures. In a recent comparative study, we have shown the capacity of 3D-MT formation for various human stem and progenitor cells relevant for cardiac cell therapy including bone-marrow (BM)-derived, adipose-derived, human embryonic stem cell-derived $Isl1^+$, or induced pluripotent stem cells [25]. Furthermore, in a previous proof-of-concept study, we demonstrated the principal feasibility and safety of a transcatheter-based intramyocardial transplantation of MSCs as 3D-MTs into the porcine heart [26]. In fact, when compared to SC cultures, several favorable features to promote tissue repair emerge within 3D-MTs when physiological cell-to-cell and cell-matrix contacts are established within their own microenvironment made of self-created extracellular matrix (ECM) [27]. Cells in 3D-MTs are organized in a highly structured manner thereby better imitating their native situation, which in return promotes their retention and engraftment [20, 26, 28–31]. Besides that, their proposed higher angiogenic potential represents another significant advantage of 3D-MTs [22, 30, 32–35]. For instance, Murphy et al. demonstrated that the secretion of vascular endothelial growth factor (VEGF), a key mediator for angiogenesis, is up to 100-fold higher in mesenchymal MSC-based 3D-MTs when compared to their SC counterparts [36].

In addition to standard in vitro methods such as tube formation, Zymogen, Transwell/Boyden chamber, and the aortic ring assays [37, 38], the chorioallantoic membrane

(CAM) of the chick embryo is a well-established assay to study angiogenesis in ovo [39, 40]. Apart from being used to test drugs for pro- and anti-angiogenic treatment [41], it has also been used in the setting of tissue engineering and regenerative medicine to investigate how different cell populations seeded within 3D biomaterials impact vessel ingrowth from the surrounding tissue [42]. Due to the immaturity of the embryonic organism, this CAM model system can be considered immune-incompetent not requiring any immunosuppressive therapy when studying human cells [40, 43]. Hence, the main advantage of this cost-efficient assay is the assessment of angiogenic activity in a model system that facilitates the translation of data from in vitro to in vivo with regard to fully functional blood vessels [44]. In addition, methods to assess quantitatively perfusion capacity in vivo by magnetic resonance imaging (MRI) are at hand [45, 46].

In the present study, we comprehensively evaluate the impact of cell format (SCs versus 3D-MTs) on the angiogenic potential of human cardiopoietic stem cells using the in ovo (in vivo) CAM assay model system (Fig. 1). In order to obtain detailed insight into their format-specific angiogenic activity and characteristics, we perform longitudinal histomorphometric evaluation on vessel formation, density, shape, and size which is then linked to an in vivo (in ovo) functionality MRI-based analysis for perfusion capacity and efficacy assessment. In addition, the impact of cell format on their tissue remodeling capacity is evaluated.

Materials and methods

Cell culture

Human cardiopoietic stem cells generated from BM-derived MSCs were isolated and processed as described elsewhere [11, 12, 15]. Briefly, BM aspirates of two adult patients were collected from the hip after obtaining written patient's consent and ethic's approval. MSCs were isolated by cultivation of BM at 37 °C and 5% CO_2 in a humidified atmosphere and by the removal of non-adherent BM cells after 24 h of incubation time. Colony forming units were isolated by a one-to-one passage (P0) and expanded for up to 6 days in DMEM high-glucose medium supplemented with 5% human pooled platelet lysate (hPL). To promote cardiopoietic differentiation, MSCs were cultured in 2.5% hPL-supplemented medium containing a cocktail of different cardiogenic growth factors as previously described [11, 12]. After cardiopoietic induction, human cardiopoietic stem cells were expanded and finally harvested by trypsinization.

All experiments were performed with culture medium consisting of DMEM high glucose (Sigma Aldrich, Switzerland) supplemented with 10% hPL (Blutspende Zurich, Switzerland), 1% penicillin/streptomycin (Gibco Life Technologies, USA), and 0.1% heparin (Bichsel, Switzerland).

3D-MT production

Cardiopoietic stem cells were trypsinized, counted (NucleoCounter, ChemoMetec A/S, Denmark), and seeded with a concentration of 1×10^4 cells/mL into Terasaki microtest plates (Greiner Bio-one, Germany). A modified hanging drop method was used to enable gravity-enforced cellular self-assembly into 3D-MTs. Briefly, 25 µL per drop of the cell culture suspension was pipetted into the 60-well Terasaki plates, which were then incubated upside down under standard conditions for 3 days. Photomicrographs of the 3D-MTs were taken to examine their morphology (Zeiss, Germany). Afterwards the 3D-MTs were harvested by washing the plates with phosphate-buffered saline (PBS; Sigma Aldrich, Switzerland) followed by centrifugation at 2000 rpm for 10 min at RT.

Scaffold seeding

The scaffold used in this study was Optimaix-3D™ (Matricel GmbH, Germany), which is a sponge made of porcine collagen. These scaffolds were proven to be biodegradable in vivo and were shown to be applicable with a broad spectrum of cell types including stem cells, making it an appropriate 3D matrix to facilitate tissue regeneration [47].

Cylindrical scaffolds (diameter: 5 mm, height: 3 mm) were seeded with 30 µL of cell suspension containing either SCs or 3D-MTs at a final concentration of 5×10^5 cells per 30 µL applied to one side of the scaffold. Subsequently, the sponges were incubated for 2 h in the incubator to allow the cells to attach before the same procedure was repeated on the opposite side of the scaffold, resulting in a total number of 1×10^6 cells per scaffold. The scaffolds were incubated for 7 days at 37 °C and 5% CO_2 in culture medium, which was changed twice a week.

CAM assay

Fertilized Lohmann white LSL chick eggs (Animalco AG Geflügelzucht, Switzerland) were incubated at 37 °C and 65% relative humidity. On incubation day (ID) 3.5, a circular window with a diameter of 40–45 mm was drilled into the eggshell after removing 2 mL albumen so that the developing CAM detached from the eggshell. The window in the eggshell was closed with a sterile petri dish of 50 mm in diameter to prevent dehydration. On ID 7, cell-seeded Optimaix-3D™ scaffolds (seeded with either 3D-MTs or with SCs) were carefully placed on top of the CAM, two scaffolds onto each egg (Fig. 2). The scaffolds were put in the middle of plastic rings (with a diameter of 1 cm) to flatten the

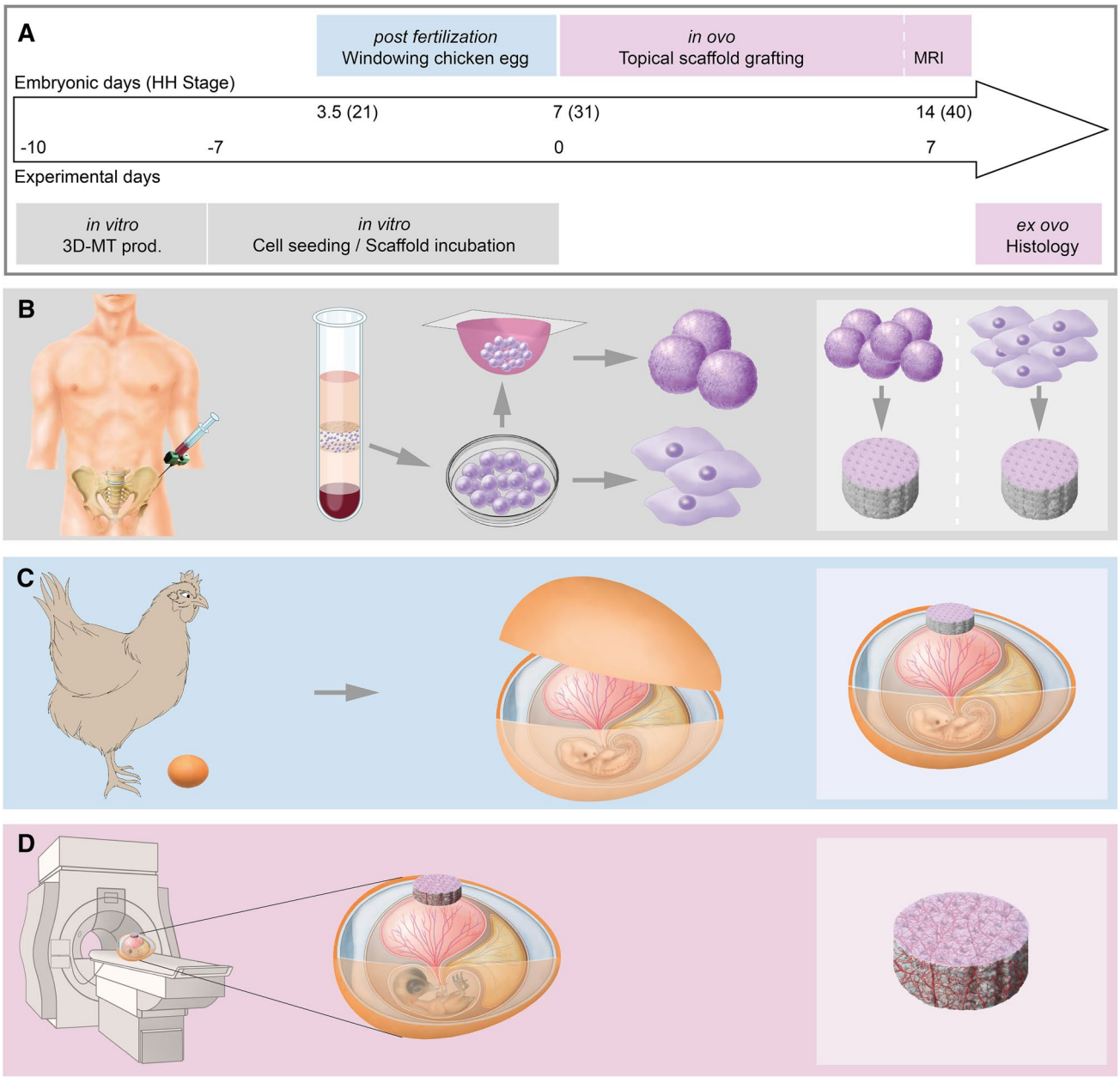

Fig. 1 Experimental setup and timeline. Detailed concept of experimental setup (**a**–**d**) with schematic timeline of the workflow (**a**). Human mesenchymal stem cells were isolated from bone marrow, differentiated into the cardiopoietic lineage and scaffolds were seeded either with generated 3D microtissues or with single cells (**b**). After the windowing of a fertilized egg, the cell-seeded scaffold was placed on top of the chorioallantoic membrane (**c**). MRI measurement of the vascularized scaffold was performed to determine the perfusion capacity followed by the quantification of the vessel density by histological examination (**d**)

surface of the CAM. Afterwards the eggs were incubated for another 7 days until ID 14.

Analysis of perfusion capacity using MRI

On ID 14, vascularization of the scaffold by capillaries of the chick embryo's CAM was studied in situ using in vivo MRI [45]. For the MRI examination, the eggs were placed onto a custom-built sliding bed and enveloped by warm water tubing to maintain the temperature of the chick embryo in a physiological range. To prevent motion of the chick embryos, they were sedated with 0.3 mL of 1:100 M medetomidine (Dorbene® *ad us. vet*., Injektionslösung, Dr. E. Graeub AG, Switzerland) dripped onto the CAM surface [48]. MRI was performed with a 4.7 T/16 cm Bruker PharmaScan small animal scanner (Bruker BioSpin, Germany)

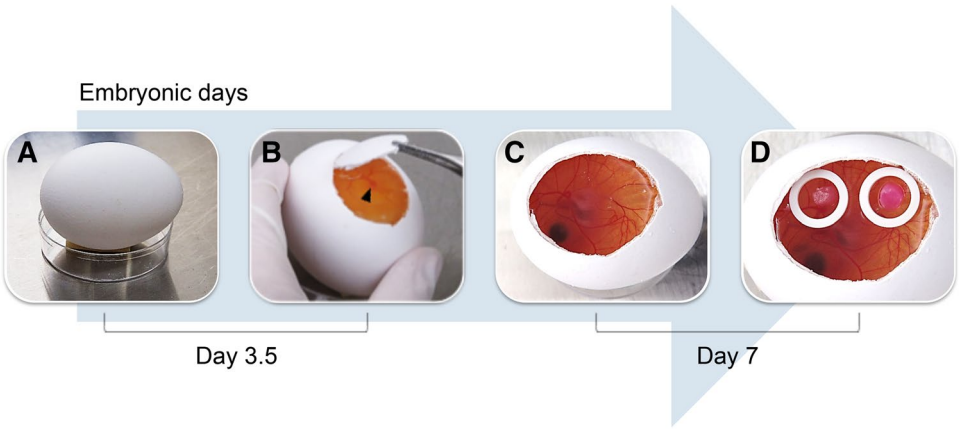

Fig. 2 Macroscopic overview of the egg preparation. Detailed process of fertilized chicken egg preparation (corresponding schematic Fig. 1c). A 2 × 3 cm piece was cut on top of the egg at embryonic day 3.5 (**a**) using the longitudinal windowing technique. The vasculature structures and the beating heart (arrow) of the embryo were visible (**b**). After incubation of additional 3.5 days, (**c**) the cell-seeded scaffolds were placed on top of the chorioallantoic membrane (**d**), either as single samples or two scaffolds in a row. At embryonic day 14, the in vivo MRI measurement and the histology processing for the determination of the vessel characteristics were performed

equipped with an actively decoupled two-coil system consisting of a 72-mm bird cage resonator for excitation and a 20-mm single-loop surface coil for reception. The surface coil was fixed on the petri dish that covered the eggshell window directly above the scaffold for optimal sensitivity.

T_1-weighted MR images were acquired with a RARE sequence of variable TR and TE for quantitative T_1 and T_2 mapping (TR 200/400/800/1500/3000/4500 ms, TE 10/30/50/70/90 ms, RARE-factor 2, image matrix size 220 × 150, field of view 45 × 30 mm^2, spatial resolution 0.2 × 0.2 mm^2, slice thickness 1 mm, total scan time 9 min 40 s). T_1 maps were acquired in four 3D-MT-seeded Optimaix-3D™ and four SC-seeded Optimaix-3D™ samples before and after i.v. injection of 100 µL 0.05 M Gd-DOTA MRI contrast agent (Dotarem®, Guerbet S.A., Switzerland). The time between Gd-DOTA injection and T_1 mapping was held constant at 25 min. T_1 relaxation times were determined in three regions of interest (ROIs) at (i) the surface of the scaffold, (ii) in the middle, and (iii) at the interface of the scaffold on the CAM. Perfusion in these three ROI was assessed through changes in the longitudinal relaxation rate, $\Delta R_1 = R_1 - R_{10}$, before and after injection of Gd-DOTA, as the relaxation rate changes with the amount of gadolinium present in the CAM:

$$R_1 = R_{10} + r_1 \cdot [\mathrm{Gd}],$$

where $R_1 = 1/T_1$ are the longitudinal relaxation rate after and R_{10} before contrast agent administration and r_1 the molar relaxivity of the contrast agent in s^{-1} mol^{-1} L and [Gd] the concentration of Gd in mol L^{-1}.

After in vivo assessment, the CAM was fixed overnight with 4% phosphate-buffered formalin solution (Formafix, Switzerland). Scaffolds together with the plastic rings were cut out (ex vivo samples), and the scaffolds were embedded in paraffin for histological analyses.

Scanning electron microscope (SEM) analysis

The scaffolds were fixed in 2% glutaraldehyde (Sigma Aldrich, Switzerland) overnight before being mounted on metal stubs with conductive double-sided tape. Samples were sputter-coated (Safematic SCD500, Bal-tec, Leica Microsystems AG, Switzerland) with platinum in order to obtain a 10 nm coating and then examined by SEM (Zeiss SUPRA 50 VP, Zeiss, UK) at an accelerating voltage of 5 kV.

Histological analysis

On ID 2, 4 and after MRI examination (ID 7) eggs were fixed overnight with 4% phosphate-buffered formalin. The scaffold–CAM complex was excised, embedded in paraffin, and sectioned at a thickness of 5 µm. Tissue sections were stained with Hematoxylin (Artechemis, Switzerland) and Eosin (Waldeck, Germany; H&E) and evaluated via stainings for CD90 (BioLegend, United Kingdom; dilution 1:80; pretreatment Tris-borate-EDTA buffer for 30 min), collagen IV (BMA Biomedicals, Switzerland; dilution 1:30; pretreatment Protease1 for 4 min), and VEGF (ThermoFisher, Switzerland; dilution 1:750; pretreatment Tris-borate-EDTA buffer for 45 min). Immunohistochemistry for CD90 and collagen IV was performed on Ventana BenchMark Ultra instruments (Ventana Medical Systems, USA) using the OptiView DAB detection kit (Roche, Switzerland), and VEGF was performed on Leica BondMax instruments using the Bond Polymer Refine Detection kit (including all buffer

solutions from Leica Microsystems Newcastle, Ltd., UK) according to manufacturer's guidelines. Images were taken with a digital slide-scanner NanoZoomer using NDP.view2 software (Hamamatsu Photonics, Japan).

Analysis of vessel characteristics

The vessel density was assessed at a magnification of ×40 by evaluating the total number of vessels present in six ROIs and three areas of each implant. The ROIs (size 0.05 mm^2) were chosen randomly at the border zone of the scaffold to the CAM, illustrating the new vessels sprouting into the scaffold. Vessels were identified morphologically by the presence of a lumen and counted manually by two independent investigators in each ROI in a blinded manner. The results were expressed as number of vessels per mm^2 (vessel density). Blood vessel size was evaluated at day 7 ex ovo. Diameters of minor and major axes, as well as circumference, of vessels were determined using ImageJ (version 1.50i) software. Thereafter, data were exported to Microsoft excel and aspect ratio ($A_R = d_{min}/d_{max}$), frequency distribution, and area (area = semi-minor axis × semi-major axis × π) were calculated. The shape factor of the vessels was examined by aspect ratio, where the value of 1 represents a circle and lower values stand for an elongated shape, like an ellipse. Mean perfusion ratio, defined as ratio of mean perfusion capacity (MPC) to total blood vessel area, was determined and the value of the SC group was set to 1.

Statistics

Vessel densities and differences in longitudinal relaxation rates were analyzed with StatView 5.0.1 software (SAS Institute Inc., USA). One-way analysis of variance (one-way ANOVA) was conducted. Pairwise comparison probabilities (p) were calculated using the Fisher's PLSD. p Values < 0.05 were considered significant and marked with *; p values < 0.01 were marked with ** and p values < 0.001 with ***. Values are presented as means ± standard deviations (SD).

Results

Generation and characterization of human cardiopoietic stem cell-derived 3D-MTs

For the generation of 3D-MTs, 250 single cardiopoietic stem cells were successfully aggregated under standardized conditions using the gravity-enforced hanging drop technique [49]. The principal feasibility of cardiopoietic stem cell-derived 3D-MT formation was observed after 24 h. After 3 days, the 3D-MTs were round shaped (Fig. 3a, b) with a diameter ranging from 44 to 72 µm (mean ± SD, 56.69 ± 8.27 µm). The 3D formation did not influence cell surface marker characteristics. Both SC suspensions of single cardiopoietic stem cells and cardiopoietic 3D-MTs were positive for the mesenchymal surface marker CD90, as well as for the ECM component collagen IV (Fig. 3c, d, g, h).

Assessment of cardiopoietic SC- or 3D-MT-seeded Optimaix-3D™ scaffolds

Histological analysis of seeded scaffolds after 7 days of cultivation in vitro showed that cardiopoietic 3D-MTs had heterogeneously migrated into the pores and were also present on the scaffold surface, whereas SCs were mainly localized in the core of the scaffold. To further analyze the surface of seeded scaffolds, SEM measurements were performed. When compared to single cardiopoietic stem cells for which a lamellar structure of the scaffold was visible, the pores of the scaffolds seeded with 3D-MTs were completely filled and covered by a layer of migrated cells from 3D-MTs into the surrounding 3D matrix (Fig. 3i, m).

Histological evaluation of angiogenic potential ex vivo (ex ovo)

In order to quantify the impact of cell format (SCs versus 3D-MTs) on angiogenic potential, the degree of neovascularization within the scaffold after seeding with either cardiopoietic SCs or 3D-MTs was analyzed by histomorphometry (Fig. 4a–d). Cross sections were stained with H&E and the number of blood vessels in the interface region was counted on days 2, 4, and 7. As expected and previously demonstrated [11, 15], an overall good angiogenic potential was detected for cardiopoietic stem cells as confirmed by substantial increase of vessel density over time for experimental both groups (SCs and 3D-MTs) (Fig. 4a). Notably, scaffolds seeded with 3D-MTs showed a significantly higher number of vessels on day 4 (122.67 ± 38.50/mm^2) and day 7 (137.44 ± 50.55/mm^2) when compared to their SC-seeded counterparts ($p \leq 0.001$ (day 4), $p \leq 0.001$ (day 7); Table 1). Interestingly, in particular small diameter vessels such as microvessels or capillaries were observed in higher frequencies for cardiopoietic 3D-MT-seeded scaffolds when compared to SCs (Fig. 4c, d).

Since it is generally known that the proangiogenic cytokine VEGF plays an important role in the migration of endothelial cells to form new branches of existing blood vessels [50], the presence of VEGF was examined immunohistochemically. The angiogenic potential of cardiopoietic 3D-MTs and single cardiopoietic stem cells was analyzed at different time points (before seeding, seeded onto scaffolds and after in ovo incubation). The cardiopoietic 3D-MTs showed a markedly higher cytoplasmic staining

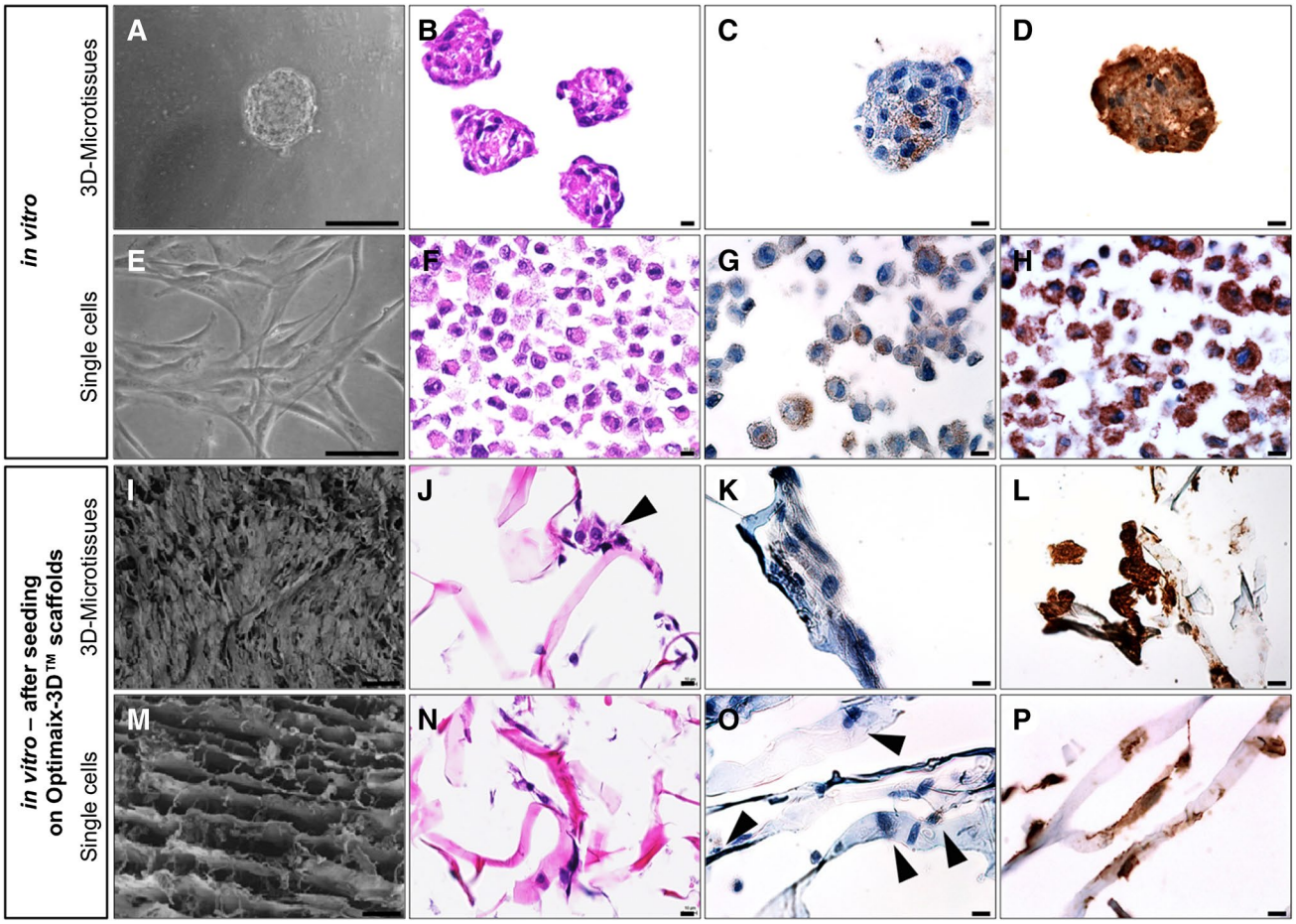

Fig. 3 Characterization of cardiopoietic 3D microtissues and single cells. Analysis of cardiopoietic 3D microtissues (**a**–**d**) and single cells (**e**–**h**) on day 3, before the scaffolds were seeded with those, by phase contrast microscopy (**a, e**), as well as H&E (**b, f, j, n**), CD90 (**c, g, k, o**), and collagen IV (**d, h, l, p**) stainings to determine cell aggregation capacity, cell surface marker profile, and ECM formation. Evaluation of static seeded Optimaix-3D™ scaffolds with either cardiopoietic 3D microtissues or single cells after 7 days of incubation (**i**–**p**). Cells seeded on the scaffold showed the same profile as observed at the time of harvesting (**k, l, o, p**). The 3D microtissues are localized in the porous structure (**j**, arrow) and on the scaffold surface, whereas single cells are homogeneously inside the scaffold (**n**). These findings were confirmed by scanning electron microscope measurements [**i, m**; scale bars: 100 µm (**a, e, i, m**) and 10 µm (**b–d, f–h, j–l, n–p**)]

intensity of VEGF than the SCs at all time points (Fig. 4e). There was no difference in staining intensity between both groups when the cells were seeded on a scaffold or not and whether the analysis was performed at in vitro or in ovo (in vivo) stages of investigation.

No inter-donor variability in regard to vessel density was identified for the 3D-MT-seeded scaffolds ($138.61 \pm 40.04/mm^2$ and $136.27 \pm 61.06/mm^2$) on day 7 (Fig. 4b). Interestingly, when kept in a SC format, the cells showed a significant difference in the quantitative analysis of vessels between donor 1 ($88.44 \pm 40.56/mm^2$) and donor 2 ($119.56 \pm 59.96/mm^2$) on day 7.

Blood vessel characteristics and functional assessment of perfusion capacity by MRI

In order to further determine the format-specific characteristics of the newly formed blood vessels, tissue sections of 3D-MT- and SC-loaded scaffolds were analyzed for vessel circumference and type of blood vessel shape. Compared to the SC group, the 3D-MT group showed an overall larger number of small blood vessels (Fig. 5a). Within the 3D-MT-loaded scaffolds, 30.8% of all vessels were in the range of 40–60 µm and 28.7% in the range of 60–80 µm, while it was only 8.0 and 17.9% in the SC counterparts. Instead, most of

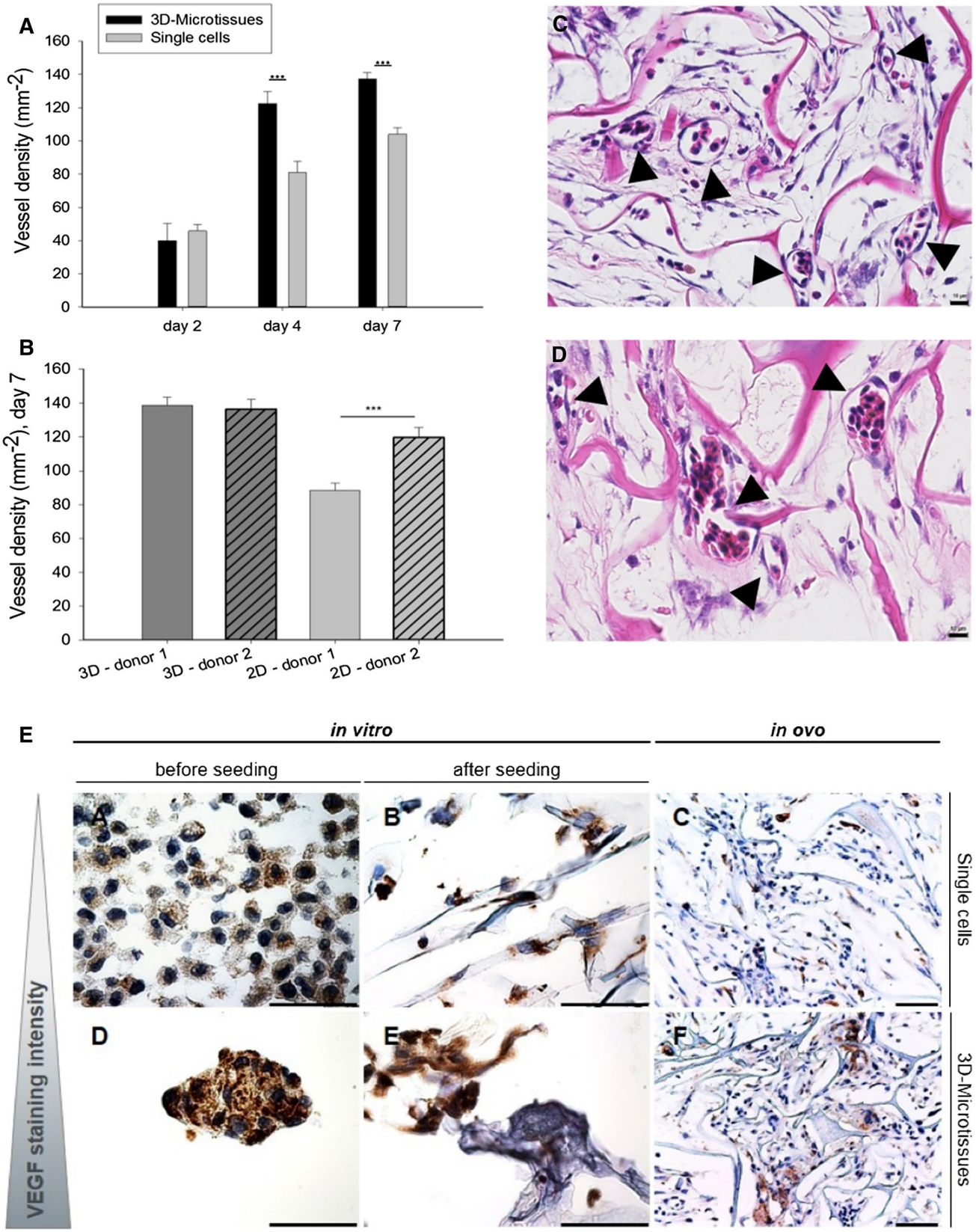
A
3D-Microtissues
Single cells
Vessel density (mm-2)
day 2
day 4
day 7
***
B
Vessel density (mm-2), day 7
3D - donor 1
3D - donor 2
2D - donor 1
2D - donor 2
C
D
E
in vitro
in ovo
before seeding
after seeding
VEGF staining intensity
Single cells
3D-Microtissues

◂**Fig. 4** Quantitative histological analysis of vessel density over a period of 7 days and vascular endothelial growth factor (VEGF) detection over time. Overall vessel density increased over time in both groups. Scaffolds seeded with cardiopoietic 3D microtissues showed a significantly higher number of vessels at day 4 and 7 when compared to their single-cell counterparts (**a**). Quantification of vessels at day 7 showed a significant difference between donors 1 and 2 for single cells, while no inter-donor variability was identified for 3D microtissue-seeded scaffolds (**b**). Data are presented as mean ± standard deviations of vessel number per square mm. One-way ANOVA was used to compare the data: ***$p < 0.001$ for 3D microtissue versus single-cell groups (**a**) and ***$p < 0.001$ for donor 1 versus donor 2 within single-cell group (**b**). Representative images of 3D microtissue-seeded (**c**) and single-cell-seeded scaffold (**d**) tissue sections to demonstrate higher number of vessels and capillaries (indicated by arrows) in the 3D microtissue-seeded scaffolds based on H&E staining. VEGF detection (**e**) of 3D microtissue-seeded scaffolds showed an increased qualitative staining intensity compared to single cells (scale bar: 10 µm)

the blood vessels in the SC group (24.1%) appeared to be larger in circumference and were in the range of 80–100 µm (Fig. 5a; Table 1). To further determine the total area of all newly formed blood vessels, the calculated areas of all individual blood vessels were added together showing that the sum (total vessel area, TVA) of the SC group vessels was approximately 1.76-fold higher when compared to the MT group (Table 1).

Next, in regard to vessel shape, 8.6% of vessels in the 3D-MT group and 7.4% in the SC group were circular (A_R 0.75–1), while 23.9% in the SC group and 29.7% in the 3D-MT group showed an elliptical shape with an A_R value of 0.5–0.75. In the range of A_R 0.25–0.5 were 68.7% of vessels in the SC group and 61.1% in the 3D-MT group, respectively. A direct correlation between the vessel size and shape became only apparent in the SC group where the larger vessels tended to have a more elliptical shape (Fig. 5b).

To further assess the newly formed capillaries and vessels in regard to their functionality, perfusion MRI was performed. The perfusion capacity was evaluated by computed value of the changes in the R_1 relaxation rates (ΔR_1) measured by MRI before and after the injection of paramagnetic Gd-DOTA contrast agent. Quantitative analysis of the ΔR_1 values within the interface, middle and surface regions of the scaffolds (Fig. 5c) showed an overall heterogeneous MPC within the whole scaffold. Interestingly, although the total area of newly formed blood vessels was substantially lower (total area of newly formed blood vessels was 1.76-fold higher in SC group), the 3D-MT group displayed a comparable perfusion capacity values when compared to the SC group (p = ns) (Fig. 5d; Table 1). In addition, also, no area-specific significant differences between the 3D-MT- and SC-loaded scaffold groups were observed at day 7 (Fig. 5d).

To compare the perfusion efficacy between groups, in a next step, the MPC was further related to the total area of newly formed blood vessels and a *perfusion ratio* (defined as the ratio of MPC to TVA) was calculated for each group. Interestingly, the *perfusion ratio* was 1.64-fold higher in the 3D-MT group suggesting superiority of vessel functionality and perfusion efficacy when compared to the SC group (Fig. 5e; Table 1).

Evaluation of tissue remodeling progress associated with neo-vessel formation

New blood vessel formation and growth is a highly orchestrated process and has also an influence on tissue healing and repair [51–53]. For this reason, the remodeling within the surrounding tissue was evaluated. A local immune response was observed during histopathological evaluation of orthotopic onplanted scaffolds (Fig. 6). H&E stained tissue sections were analyzed for evidence of a tissue remodeling process and indeed, when compared to SC-loaded scaffolds most of the 3D-MT-seeded scaffolds showed a strong cell infiltration at day 3 and 7 (Fig. 6a, d, e) and an increased presence of multi-nucleated giant cells (Fig. 6c). The infiltrated cells could be identified as heterophilic phenotype, followed by cells of mesenchymal origin like fibroblasts. Collagen deposition was detected by immunohistochemical staining for collagen IV (Fig. 6d–g) and an increase in collagen was observed in both groups over time. Interestingly, in the 3D-MT group, an intense accumulation of collagen was already seen at day 3 suggesting a stronger tissue remodeling response (Fig. 6d) when compared to the SC-seeded scaffolds (Fig. 6f).

Taken together, particularly in the cardiopoietic 3D-MT group we observed a distinct tissue remodeling process (Table 1), which is based on gradual cell infiltration and development of neo-vessels, followed by progressive collagen deposition.

Discussion

Besides the selection of the ideal cell type, the application format by which cell are delivered to the target has been suggested to play an important role in the therapeutic efficacy of current cell therapy concepts [20, 25, 26, 30, 36].

In this study, we compared the impact of cell format (SCs versus 3D-MTs) on the angiogenic potential of human cardiopoietic stem cells, an encouraging next-generation cell type for cardiac repair [5, 11–15, 54, 55]. To evaluate the impact of cell format on the angiogenic activity and its subsequent neo-vessel formation and functionality, both cell formats were seeded onto porous biodegradable collagen scaffolds, which were then placed on the CAM of living chicken embryos and analyzed for their perfusion capacity of the newly ingrown vessels by MRI after 1 week. In parallel, format-specific blood vessel density and characteristics were

Table 1 Impact of cell format (single cells versus 3D microtissues) on angiogenic potential of cardiopoietic stem cells

Cell type	Assessment		Cell format	
Cardiopoietic stem cells	Histology	MRI	3D microtissues	Single cells
Vessel density	X		↑	↓
Microvessel frequency	X		↑	↓
Total vessel area	X		↓	↑
Perfusion capacity		X	→	→
Perfusion ratio	X	X	↑	↓
Tissue remodeling	X		↑	↓

Analysis pattern of vessel ingrowth and functionality (both day 7) to evaluate the comparison of scaffolds seeded with 3D microtissues or single cells (↑ = increased frequency compared to the other group, ↓ = lower occurrence compared to the other group, → = comparable frequency in both groups)

Fig. 5 Extended quantitative histological examination of blood vessels and assessment of perfusion capacity by MRI. Histological sections were evaluated for vessel circumference (**a**) to identify potentially microvessels within scaffolds with 3D microtissue and single-cell seeding, respectively. The tissue samples of the 3D microtissue group tend to have an increased frequency of a smaller circumference and a more uniform shape (**b**) than samples of the single-cell group. All vessels of 3D microtissue-loaded scaffolds correspond with 39% to an A_R of 0.5–1 compared to 31% of single-cell-loaded scaffolds. In the correlation of the size of blood vessels to their shape, the single-cell group showed an increased irregularity of shape in the large-volume vessels, while the 3D microtissue group showed no tendency in this respect (**b**). Despite differences in vessel density, size, and area, quantitative MRI analysis of ΔR_1 values within the interface, middle, and surface regions of the scaffolds (**c**; scale bar: 0.5 cm) showed no significant differences between the 3D microtissue and single-cell-loaded scaffold groups after 7 days of incubation on the chorioallantoic membrane (**d**). The perfusion ratio and functionality, defined as mean perfusion capacity in relation to total blood vessel area, is higher in the 3D microtissue group compared to the single-cell group (**e**)

further assessed by longitudinal histomorphometry ex vivo (ex ovo) and linked to the perfusion analysis.

Our histomorphometric analysis showed that cellular self-assembly of cardiopoietic stem cells into 3D-MTs leads to a significant increase of vessel density after 4 and 7 days on the CAM when compared to SC-seeded scaffolds suggesting that cellular self-assembly into 3D-MTs substantially enhances the angiogenic activity of cardiopoietic stem cells. Moreover, our data demonstrated that this was mainly driven by, an overall higher number of neo-capillary formation when compared to the SC group. To the contrary, SC-seeded scaffolds showed a higher frequency of larger vessels resulting in an overall higher total area of newly formed blood vessels (1.76-fold higher). Remarkably, and despite the substantial difference in TVA, the perfusion capacity was similar in both groups therefore suggesting functional superiority together with an enhanced perfusion efficacy of the neo-vessels formed in 3D-MT-seeded scaffolds. This was further underlined by a 1.64-fold higher *perfusion ratio* in the 3D-MT group. Taken together, our results show that cellular self-assembly of human cardiopoietic stem cells into a 3D cell format (3D-MTs) may substantially (1) enhance their overall angiogenic activity and potential; and (2) impact neo-vessel characteristics and their functionality (Table 1).

Importantly, our study also highlights that the sole morphological evaluation on angiogenesis and neo-vessel formation cannot discriminate between functional and non-functional neo-vessels, and may therefore be not sufficient enough when evaluating stem cells or other biologics (i.e., microRNAs or exosomes) for their therapeutic angiogenic potential. Hence, it is always important to relate the morphological ex vivo evaluation with an in vivo assessment to determine the true therapeutic potential when studying angiogenesis neovascularization.

To salvage ischemic myocardium at early stages after MI, de novo formation of microvessels and increase of capillary density are crucial factors to preserve heart function and to prevent the transition to heart failure [56–60]. Hence, from a therapeutic perspective the strategy of assembling stem cells into 3D-MTs prior to transplantation into the diseased heart may increase their tissue repair capacity, in particular, since the majority of current clinical cardiac cell therapy strategies primarily relies on paracrine effects which are strongly based on angiogenic effects [5, 61].

Besides the application format by which cells are delivered to the target organ, the selection of the ideal cell type plays a crucial role in current therapy concepts. In our study, we used human BM-derived MSCs, which underwent lineage specification towards a cardiac committed phenotype (guided cardiopoiesis), using a cardiogenic cocktail, in order to enhance their cardioreparative properties [6, 9, 11, 62]. Based on encouraging data from murine ischemic cardiomyopathy models [11], the concept of cardiopoietic stem cells was rapidly advanced into humans and is currently undergoing systematic clinical investigation in several randomized, multicenter trials [12–14, 55]. Moreover, in a recent report using a pig model of post-infarction LV dysfunction, we demonstrated the therapeutic efficacy of human cardiopoietic stem cells following transcatheter intramyocardial delivery [15]. We showed that when delivered in the subacute phase of infarction cardiopoietic cell therapy leads to functional recovery and efficiently prevents from negative LV remodeling. Interestingly, the overall intramyocardial integration of cardiopoietic cells appeared to be very limited 30 days after transplantation suggesting that the observed therapeutic effect was primarily due to substantial angiogenic effects driven by paracrine mechanisms. In fact, the strong angiogenic potential of cardiopoietic stem cells was

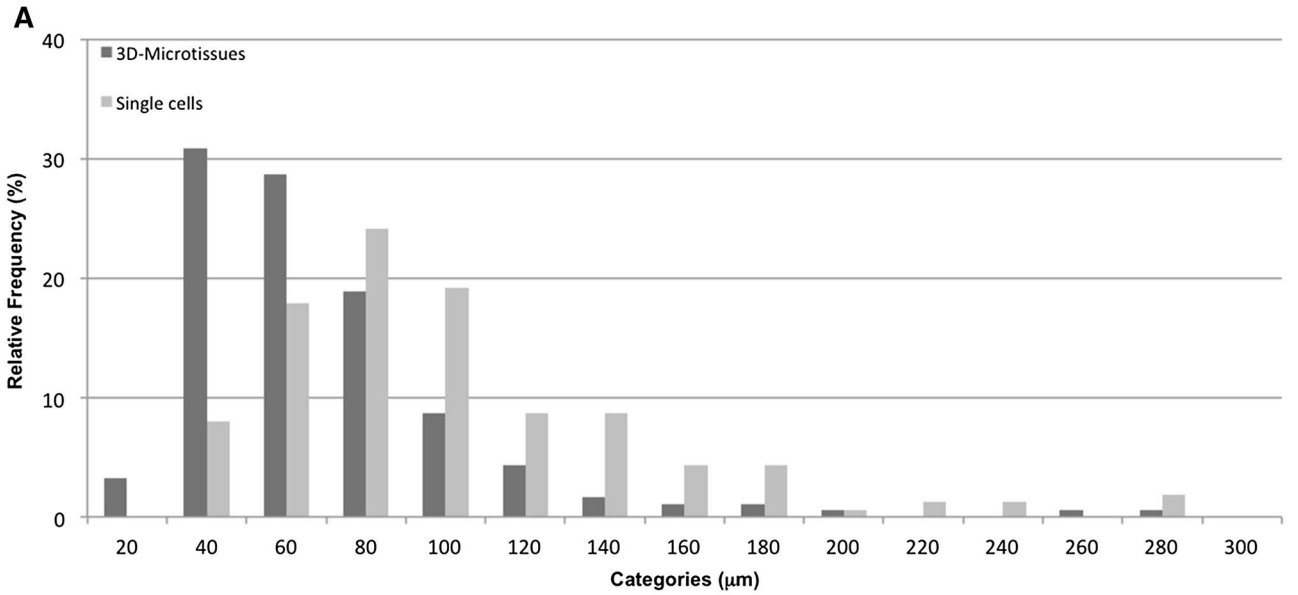
A
3D-Microtissues
Single cells
Relative Frequency (%)
0
10
20
30
40
20
40
60
80
100
120
140
160
180
200
220
240
260
280
300
Categories (μm)

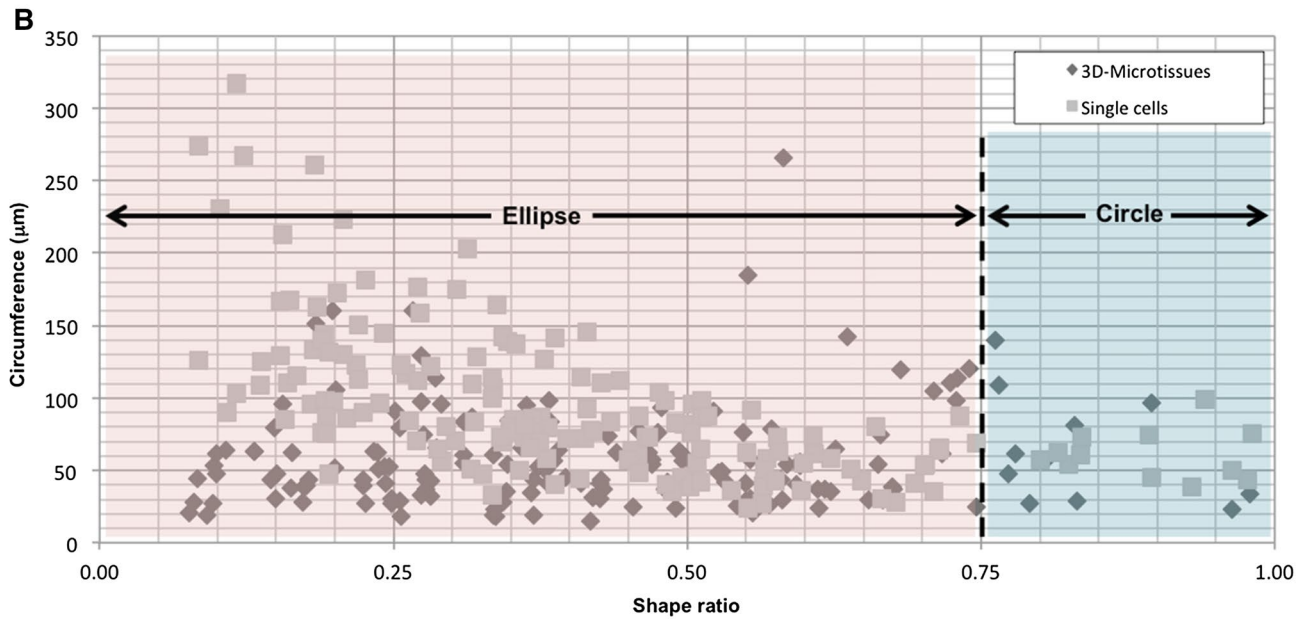
B
3D-Microtissues
Single cells
Ellipse
Circle
Circumference (μm)
0
50
100
150
200
250
300
350
0.00
0.25
0.50
0.75
1.00
Shape ratio

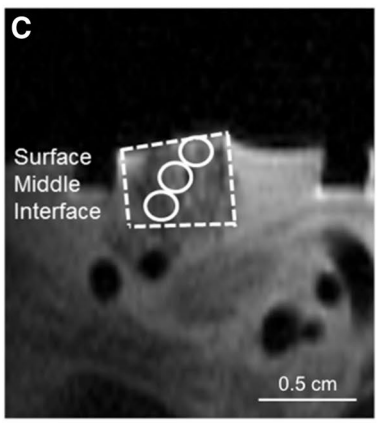
C
Surface
Middle
Interface
0.5 cm

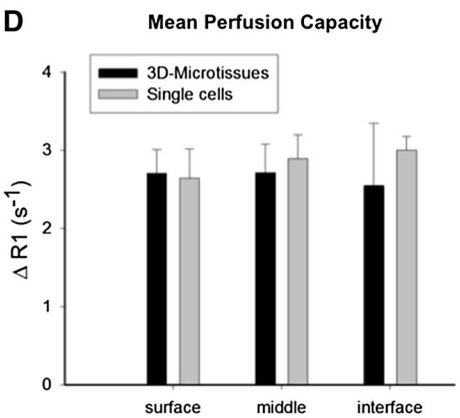
D
Mean Perfusion Capacity
3D-Microtissues
Single cells
Δ R1 (s-1)
0
1
2
3
4
surface
middle
interface

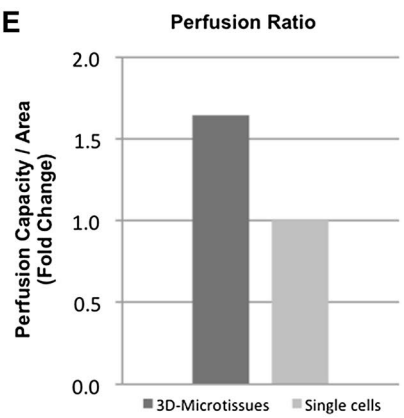
E
Perfusion Ratio
Perfusion Capacity / Area (Fold Change)
0.0
0.5
1.0
1.5
2.0
3D-Microtissues
Single cells

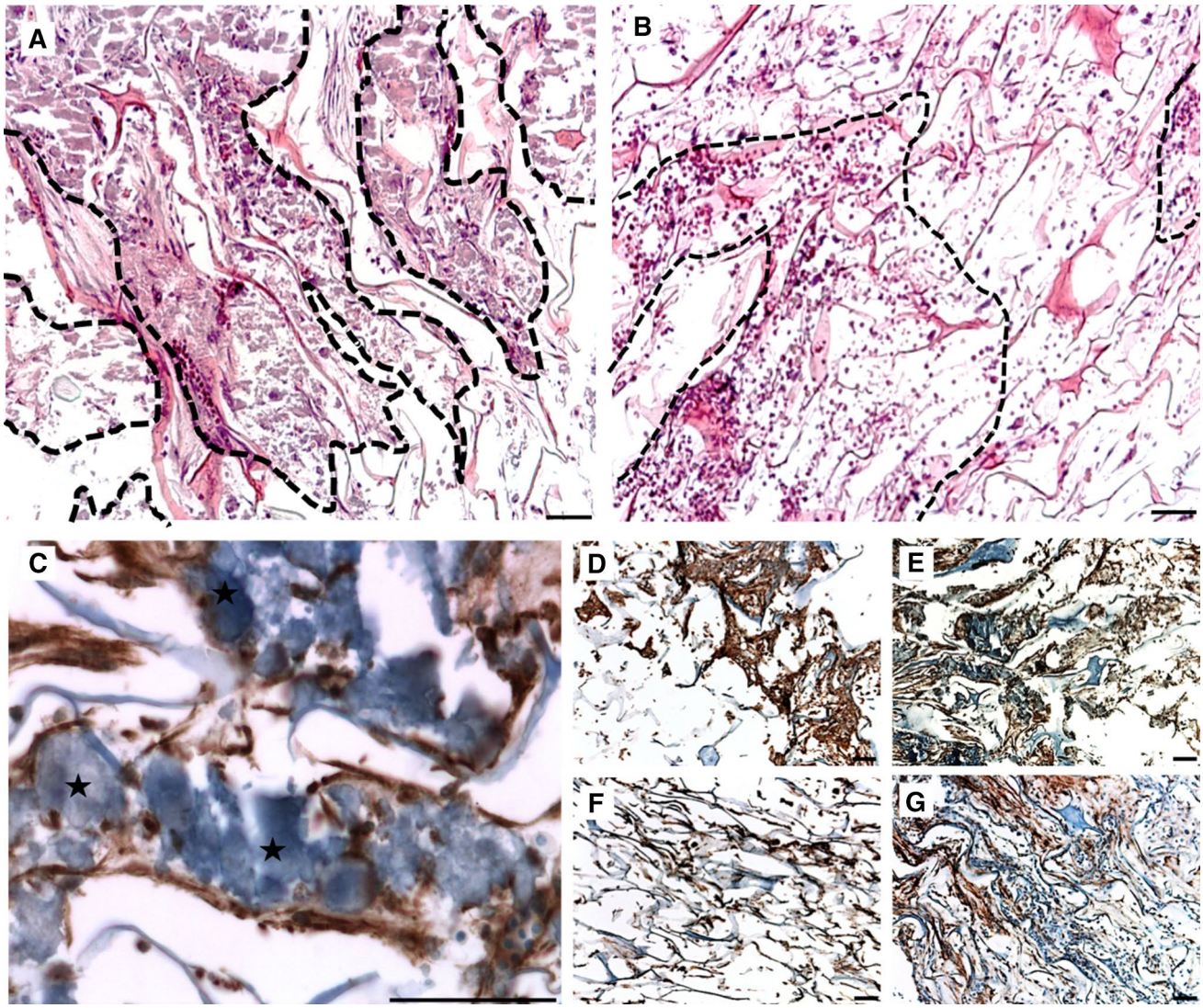

Fig. 6 Histological examination of tissue remodeling based on H&E and collagen IV staining. H&E stained tissue sections (**a, b**) from scaffolds seeded with 3D microtissues showed a strong cellular infiltration at day 7 (**a**) and in addition a massive collagen deposition at day 3 (**d**) and day 7 (**e**), which was detected by collagen IV staining. Areas of tissue ingrowth, from the chorioallantoic membrane into the pores of the scaffold, are outlined and visualized by dashed lines (**a, b**) in the tissue section samples stained with H&E. The presence of multi-nucleated giant cells (**c**, asterisks) was detected in collagen IV stained 3D microtissue-seeded scaffolds. Tissues of the single-cell-loaded scaffold group (**b**) demonstrated a limited remodeling degree based on collagen IV staining at day 3 (**f**) and day 7 (**g**) compared to the 3D microtissue-seeded scaffold group (scale bars: 50 µm)

proven in this study in vitro and ex vivo (post-mortem) using tube formation assays prior to transplantation (in vitro) and a by significantly increased von Willebrand Factor^{+} vessel density in the border zone of the infarction (ex vivo) [15].

These data are in line with our current findings as in both groups (SC- and 3D-MT-seeded scaffolds), an increase of vessel density over time together with a good perfusion capacity was seen confirming the overall strong angiogenic potential of cardiopoietic stem cells. Notably, and beyond that, 3D-MT-seeded scaffolds exhibited a significantly enhanced (micro)vessel density along with an increased functionality and perfusion efficacy when compared to their SC counterparts.

Hence, cellular self-assembly of cardiopoietic stem cells into 3D-MTs may further increase their cardioreparative properties and their therapeutic potential. Therefore, further evaluation of cardiopoietic stem cell-derived 3D-MTs in preclinical large animal studies may be warranted. Indeed, in a recent *proof-of-concept* study we were able to demonstrate the safety and feasibility of a transcatheter-based intramyocardial transplantation of human MSC-based 3D-MTs into the porcine heart [26].In general, the concept

of 3D cell aggregation into spheroids or MTs to enhance therapeutic efficacy in cell-based therapies has gained considerable attention [20, 63–65] and various cell types have been systematically characterized for their capacity to form 3D-MTs [25]. Indeed, when compared to SCs, the superiority of 3D-MTs is multifactorial as they (1) provide a more physiological environment; (2) better resemble the natural stem cell niche; (3) stronger mimic natural tissue due to the formation of structural ECM; and (4) provide favorable adhesion characteristics, which is crucial to achieve improved integration and engraftment in the setting of cell therapeutic approaches [20].

However, to date, there are only very few reports that have evaluated their impact on neoangiogenesis. Laschke and coworkers studied the angiogenic effects of murine adipose-derived stem cell-derived 3D-MTs, which were pre-differentiated towards an endothelial cell type, that were seeded into a porous polyurethane scaffold and assessed in the dorsal skinfold chamber. They found that the spheroids acted as initiators of blood vessel formation within this scaffold [66]. Next, Murphy and coworkers showed to achieve a 100 times higher the secretion of VEGF when assembling MSCs into 3D-MTs [36].

Finally, our study also revealed advantages in regard to tissue remodeling when assembling cardiopoietic stem cells into 3D-MTs before seeding. 3D-MTs led to a much higher degree of ingrowth and tissue formation by substantial infiltration and filling of the collagen scaffold pores. This process was accompanied by the production of more ground substance (active amorphous tissue) as well as the mobilization of numerous heterophils and blood building plasma cells. Moreover, on a qualitative level, increased numbers of foreign body giant cells were detected at the interface of the scaffold to the tissue of the CAM. This abundant tissue infiltration was further characterized by the presence apoptotic and necrotic cells—and at the same time by vital fibroblasts. Taken together, enhanced collagen deposition along with more foreign body giant cells were present in the interface region in the 3D-MT-seeded scaffolds when compared to their SC counterparts suggesting a cell-format-driven enhanced tissue remodeling.

Limitations

Our study has several limitations: First, the CAM assay allows analysis of neovascularization in a restricted time frame of 7 days only. Second, the angiogenic advantage of 3D-MTs over SCs found can only be attributed to cardiopoietic stem cells, while it remains to be validated for other cell types. Third, a comprehensive histological analysis is challenging due to a lack of specific antibodies for chicken tissue. Fourth, the assessment strategy of the ROIs may have impacted the results on vessel characteristics to some extent. However, a potential bias was minimized by performing the analysis in a blinded fashion and by two independent investigators. Finally, as a result of grafting, there might be also a non-specific inflammatory reaction (to some extent) inducing an additional vasoproliferative response, which may potentially impede the primary (main) response [67–69].

Conclusions

In summary, when compared to classical SC suspensions, our study demonstrates that cellular self-assembly of human cardiopoietic stem cells into 3D-MTs substantially increases their overall angiogenic potential as well as their functional revascularization capacity. In line with that, our data also displayed an enhanced tissue remodeling capacity when assembling cardiopoietic stem cells into 3D-MTs before seeding. These findings warrant further evaluation in preclinical large animal studies which may build the basis for future clinical translation.

Acknowledgements We thank Carol De Simio for her excellent graphical support (University Hospital Zurich, Switzerland). We additionally thank André Fitsche, Christiane Mittmann, Ursula Süss, and Pia Fuchs for great support on histological processing (Institute of Pathology and Department of Surgical Research, University Hospital Zurich, Switzerland). Fatma Kivrak Pfiffner is acknowledged for technical assistance with the handling of the eggs (Clinic for Plastic Surgery and Hand Surgery, University Hospital Zurich, Switzerland). We kindly thank Peter De Weale, Aymeric Seron, Dorothee Daro, and Sebastien Mauen (Celyad, Belgium) for generation of the GMP-grade human cardiopoietic stem cells.

Author contributions PW, JB, and MYE designed experiments; PW, AB, AW, and JB performed experiments; PW, AB, JB, and MYE analyzed all data; YT injected contrast agent for MRI measurements; OE performed SEM; MH evaluated all histological sections; PW, AB, JB, and MYE wrote manuscript; PW, AB, AW, MH, PG, MC, SPH, JB, and MYE edited and discussed manuscript.

Funding This work was supported by the Hartmann Müller-Foundation and the Swiss Heart Foundation.

Compliance with ethical standards

Conflict of interest The authors declare that they have no competing interests.

References

1. Nelson TJ, Behfar A, Terzic A (2008) Strategies for therapeutic repair: the "R(3)" regenerative medicine paradigm. Clin Transl Sci 1:168–171
2. Terzic A, Pfenning MA, Gores GJ, Harper CM Jr (2015) Regenerative medicine build-out. Stem Cells Transl Med 4:1373–1379

3. Tsukamoto A, Abbot SE, Kadyk LC, DeWitt ND, Schaffer DV, Wertheim JA, Whittlesey KJ, Werner MJ (2016) Challenging regeneration to transform medicine. Stem Cells Transl Med 5:1–7
4. Segers VF, Lee RT (2008) Stem-cell therapy for cardiac disease. Nature 451:937–942
5. Cambria E, Pasqualini FS, Wolint P, Gunter J, Steiger J, Bopp A, Hoerstrup SP, Emmert MY (2017) Translational cardiac stem cell therapy: advancing from first-generation to next-generation cell types. NPJ Regen Med 2:17
6. Behfar A, Terzic A (2014) Stem cell in the rough: repair quotient mined out of a bone marrow niche. Circ Res 115:814–816
7. Gyongyosi M, Wojakowski W, Lemarchand P, Lunde K, Tendera M, Bartunek J, Marban E, Assmus B, Henry TD, Traverse JH, Moye LA, Surder D, Corti R, Huikuri H, Miettinen J, Wohrle J, Obradovic S, Roncalli J, Malliaras K, Pokushalov E, Romanov A, Kastrup J, Bergmann MW, Atsma DE, Diederichsen A, Edes I, Benedek I, Benedek T, Pejkov H, Nyolczas N, Pavo N, Bergler-Klein J, Pavo IJ, Sylven C, Berti S, Navarese EP, Maurer G, Investigators A (2015) Meta-Analysis of Cell-based CaRdiac stUdiEs (ACCRUE) in patients with acute myocardial infarction based on individual patient data. Circ Res 116:1346–1360
8. Marban E, Malliaras K (2012) Mixed results for bone marrow-derived cell therapy for ischemic heart disease. JAMA 308:2405–2406
9. Behfar A, Faustino RS, Arrell DK, Dzeja PP, Perez-Terzic C, Terzic A (2008) Guided stem cell cardiopoiesis: discovery and translation. J Mol Cell Cardiol 45:523–529
10. Marban E, Malliaras K (2010) Boot camp for mesenchymal stem cells. J Am Coll Cardiol 56:735–737
11. Behfar A, Yamada S, Crespo-Diaz R, Nesbitt JJ, Rowe LA, Perez-Terzic C, Gaussin V, Homsy C, Bartunek J, Terzic A (2010) Guided cardiopoiesis enhances therapeutic benefit of bone marrow human mesenchymal stem cells in chronic myocardial infarction. J Am Coll Cardiol 56:721–734
12. Bartunek J, Behfar A, Dolatabadi D, Vanderheyden M, Ostojic M, Dens J, El Nakadi B, Banovic M, Beleslin B, Vrolix M, Legrand V, Vrints C, Vanoverschelde JL, Crespo-Diaz R, Homsy C, Tendera M, Waldman S, Wijns W, Terzic A (2013) Cardiopoietic stem cell therapy in heart failure: the C-CURE (Cardiopoietic stem Cell therapy in heart failURE) multicenter randomized trial with lineage-specified biologics. J Am Coll Cardiol 61:2329–2338
13. Bartunek J, Davison B, Sherman W, Povsic T, Henry TD, Gersh B, Metra M, Filippatos G, Hajjar R, Behfar A, Homsy C, Cotter G, Wijns W, Tendera M, Terzic A (2016) Congestive Heart Failure Cardiopoietic Regenerative Therapy (CHART-1) trial design. Eur J Heart Fail 18:160–168
14. Bartunek J, Terzic A, Davison BA, Filippatos GS, Radovanovic S, Beleslin B, Merkely B, Musialek P, Wojakowski W, Andreka P, Horvath IG, Katz A, Dolatabadi D, El Nakadi B, Arandjelovic A, Edes I, Seferovic PM, Obradovic S, Vanderheyden M, Jagic N, Petrov I, Atar S, Halabi M, Gelev VL, Shochat MK, Kasprzak JD, Sanz-Ruiz R, Heyndrickx GR, Nyolczas N, Legrand V, Guedes A, Heyse A, Moccetti T, Fernandez-Aviles F, Jimenez-Quevedo P, Bayes-Genis A, Hernandez-Garcia JM, Ribichini F, Gruchala M, Waldman SA, Teerlink JR, Gersh BJ, Povsic TJ, Henry TD, Metra M, Hajjar RJ, Tendera M, Behfar A, Alexandre B, Seron A, Stough WG, Sherman W, Cotter G, Wijns W, CHART Program (2017) Cardiopoietic cell therapy for advanced ischaemic heart failure: results at 39 weeks of the prospective, randomized, double blind, sham-controlled CHART-1 clinical trial. Eur Heart J 38:648–660
15. Emmert MY, Wolint P, Jakab A, Sheehy SP, Pasqualini FS, Nguyen TD, Hilbe M, Seifert B, Weber B, Brokopp CE, Macejovska D, Caliskan E, von Eckardstein A, Schwartlander R, Vogel V, Falk V, Parker KK, Gyongyosi M, Hoerstrup SP (2017) Safety and efficacy of cardiopoietic stem cells in the treatment of post-infarction left-ventricular dysfunction—from cardioprotection to functional repair in a translational pig infarction model. Biomaterials 122:48–62
16. Laflamme MA, Murry CE (2005) Regenerating the heart. Nat Biotechnol 23:845–856
17. Alrefai MT, Murali D, Paul A, Ridwan KM, Connell JM, Shum-Tim D (2015) Cardiac tissue engineering and regeneration using cell-based therapy. Stem Cells Cloning 8:81–101
18. Radisic M, Christman KL (2013) Materials science and tissue engineering: repairing the heart. Mayo Clin Proc 88:884–898
19. Haraguchi Y, Shimizu T, Yamato M, Okano T (2012) Concise review: cell therapy and tissue engineering for cardiovascular disease. Stem Cells Transl Med 1:136–141
20. Gunter J, Wolint P, Bopp A, Steiger J, Cambria E, Hoerstrup SP, Emmert MY (2016) Microtissues in cardiovascular medicine: regenerative potential based on a 3D microenvironment. Stem Cells Int 9098523
21. Alajati A, Laib AM, Weber H, Boos AM, Bartol A, Ikenberg K, Korff T, Zentgraf H, Obodozie C, Graeser R, Christian S, Finkenzeller G, Stark GB, Heroult M, Augustin HG (2008) Spheroid-based engineering of a human vasculature in mice. Nat Methods 5:439–445
22. Bhang SH, Lee S, Shin JY, Lee TJ, Kim BS (2012) Transplantation of cord blood mesenchymal stem cells as spheroids enhances vascularization. Tissue Eng A 18:2138–2147
23. Lee GH, Lee JS, Wang X, Lee SH (2016) Bottom-up engineering of well-defined 3D microtissues using microplatforms and biomedical applications. Adv Healthc Mater 5:56–74
24. Metzger W, Sossong D, Bachle A, Putz N, Wennemuth G, Pohlemann T, Oberringer M (2011) The liquid overlay technique is the key to formation of co-culture spheroids consisting of primary osteoblasts, fibroblasts and endothelial cells. Cytotherapy 13:1000–1012
25. Emmert MY, Wolint P, Wickboldt N, Gemayel G, Weber B, Brokopp CE, Boni A, Falk V, Bosman A, Jaconi ME, Hoerstrup SP (2013) Human stem cell-based three-dimensional microtissues for advanced cardiac cell therapies. Biomaterials 34:6339–6354
26. Emmert MY, Wolint P, Winklhofer S, Stolzmann P, Cesarovic N, Fleischmann T, Nguyen TD, Frauenfelder T, Boni R, Scherman J, Bettex D, Grunenfelder J, Schwartlander R, Vogel V, Gyongyosi M, Alkadhi H, Falk V, Hoerstrup SP (2013) Transcatheter based electromechanical mapping guided intramyocardial transplantation and in vivo tracking of human stem cell based three dimensional microtissues in the porcine heart. Biomaterials 34:2428–2441
27. Fennema E, Rivron N, Rouwkema J, van Blitterswijk C, de Boer J (2013) Spheroid culture as a tool for creating 3D complex tissues. Trends Biotechnol 31:108–115
28. Cheng NC, Wang S, Young TH (2012) The influence of spheroid formation of human adipose-derived stem cells on chitosan films on stemness and differentiation capabilities. Biomaterials 33:1748–1758
29. Emmert MY, Hitchcock RW, Hoerstrup SP (2014) Cell therapy, 3D culture systems and tissue engineering for cardiac regeneration. Adv Drug Deliv Rev 69–70:254–269
30. Kim JH, Park IS, Park Y, Jung Y, Kim SH, Kim SH (2013) Therapeutic angiogenesis of three-dimensionally cultured adipose-derived stem cells in rat infarcted hearts. Cytotherapy 15:542–556
31. Lee WY, Wei HJ, Lin WW, Yeh YC, Hwang SM, Wang JJ, Tsai MS, Chang Y, Sung HW (2011) Enhancement of cell retention and functional benefits in myocardial infarction using human amniotic-fluid stem-cell bodies enriched with endogenous ECM. Biomaterials 32:5558–5567
32. Kapur SK, Wang X, Shang H, Yun S, Li X, Feng G, Khurgel M, Katz AJ (2012) Human adipose stem cells maintain

proliferative, synthetic and multipotential properties when suspension cultured as self-assembling spheroids. Biofabrication 4:025004
33. Kelm JM, Ehler E, Nielsen LK, Schlatter S, Perriard JC, Fussenegger M (2004) Design of artificial myocardial microtissues. Tissue Eng 10:201–214
34. Oltolina F, Zamperone A, Colangelo D, Gregoletto L, Reano S, Pietronave S, Merlin S, Talmon M, Novelli E, Diena M, Nicoletti C, Musaro A, Filigheddu N, Follenzi A, Prat M (2015) Human cardiac progenitor spheroids exhibit enhanced engraftment potential. PLoS ONE 10:e0137999
35. Tseliou E, Pollan S, Malliaras K, Terrovitis J, Sun B, Galang G, Marban L, Luthringer D, Marban E (2013) Allogeneic cardiospheres safely boost cardiac function and attenuate adverse remodeling after myocardial infarction in immunologically mismatched rat strains. J Am Coll Cardiol 61:1108–1119
36. Murphy KC, Fang SY, Leach JK (2014) Human mesenchymal stem cell spheroids in fibrin hydrogels exhibit improved cell survival and potential for bone healing. Cell Tissue Res 357:91–99
37. Adair TH, Montani JP (2010) Angiogenesis assays. In: Sciences MCL (ed) Angiogenesis. Morgan & Claypool Publishers, San Rafael
38. Goodwin AM (2007) In vitro assays of angiogenesis for assessment of angiogenic and anti-angiogenic agents. Microvasc Res 74:172–183
39. Ribatti D (2008) Chick embryo chorioallantoic membrane as a useful tool to study angiogenesis. Int Rev Cell Mol Bio 270:181–224
40. Ribatti D, Vacca A, Roncali L, Dammacco F (1996) The chick embryo chorioallantoic membrane as a model for in vivo research on angiogenesis. Int J Dev Biol 40:1189–1197
41. Gokce G, Ozgurtas T, Sobaci G, Kucukevcilioglu M (2016) The effects of amphotericin B on angiogenesis in chick chorioallantoic membrane. Cutan Ocul Toxicol 35:92–96
42. Woloszyk A, Buschmann J, Waschkies C, Stadlinger B, Mitsiadis TA (2016) Human dental pulp stem cells and gingival fibroblasts seeded into silk fibroin scaffolds have the same ability in attracting vessels. Front Physiol 7:140
43. Borges J, Tegtmeier FT, Padron NT, Mueller MC, Lang EM, Stark GB (2003) Chorioallantoic membrane angiogenesis model for tissue engineering: a new twist on a classic model. Tissue Eng 9:441–450
44. Staton CA, Reed MW, Brown NJ (2009) A critical analysis of current in vitro and in vivo angiogenesis assays. Int J Exp Pathol 90:195–221
45. Kivrak Pfiffner F, Waschkies C, Tian Y, Woloszyk A, Calcagni M, Giovanoli P, Rudin M, Buschmann J (2015) A new in vivo magnetic resonance imaging method to noninvasively monitor and quantify the perfusion capacity of three-dimensional biomaterials grown on the chorioallantoic membrane of chick embryos. Tissue Eng C 21:339–346
46. Zuo Z, Syrovets T, Genze F, Abaei A, Ma G, Simmet T, Rasche V (2015) High-resolution MRI analysis of breast cancer xenograft on the chick chorioallantoic membrane. NMR Biomed 28:440–447
47. GmbH M (2017) Optimaix scaffolds for cell culture research
48. Waschkies C, Nicholls F, Buschmann J (2015) Comparison of medetomidine, thiopental and ketamine/midazolam anesthesia in chick embryos for in ovo Magnetic Resonance Imaging free of motion artifacts. Sci Rep 5:15536
49. Kelm JM, Timmins NE, Brown CJ, Fussenegger M, Nielsen LK (2003) Method for generation of homogeneous multicellular tumor spheroids applicable to a wide variety of cell types. Biotechnol Bioeng 83:173–180
50. Kastellorizios M, Papadimitrakopoulos F, Burgess DJ (2015) Multiple tissue response modifiers to promote angiogenesis and prevent the foreign body reaction around subcutaneous implants. J Controlled Release 214:103–111
51. Dondossola E, Holzapfel BM, Alexander S, Filippini S, Hutmacher DW, Friedl P (2016) Examination of the foreign body response to biomaterials by nonlinear intravital microscopy. Nat Biomed Eng 1
52. Logsdon EA, Finley SD, Popel AS, Mac Gabhann F (2014) A systems biology view of blood vessel growth and remodelling. J Cell Mol Med 18:1491–1508
53. Silvestre JS, Levy BI, Tedgui A (2008) Mechanisms of angiogenesis and remodelling of the microvasculature. Cardiovasc Res 78:201–202
54. Cambria E, Steiger J, Gunter J, Bopp A, Wolint P, Hoerstrup SP, Emmert MY (2016) Cardiac regenerative medicine: the potential of a new generation of stem cells. Transfus Med Hemother 43:275–281
55. Teerlink JR, Metra M, Filippatos GS, Davison BA, Bartunek J, Terzic A, Gersh BJ, Povsic TJ, Henry TD, Alexandre B, Homsy C, Edwards C, Seron A, Wijns W, Cotter G, Investigators C (2017) Benefit of cardiopoietic mesenchymal stem cell therapy on left ventricular remodelling: results from the Congestive Heart Failure Cardiopoietic Regenerative Therapy (CHART-1) study. Eur J Heart Fail 19:1520–1529
56. Cochain C, Channon KM, Silvestre JS (2013) Angiogenesis in the infarcted myocardium. Antioxid Redox Signal 18:1100–1113
57. Vilahur G, Onate B, Cubedo J, Bejar MT, Arderiu G, Pena E, Casani L, Gutierrez M, Capdevila A, Pons-Llado G, Carreras F, Hidalgo A, Badimon L (2017) Allogenic adipose-derived stem cell therapy overcomes ischemia-induced microvessel rarefaction in the myocardium: systems biology study. Stem Cell Res Ther 8:52
58. Ji ST, Kim H, Yun J, Chung JS, Kwon SM (2017) Promising therapeutic strategies for mesenchymal stem cell-based cardiovascular regeneration: from cell priming to tissue engineering. Stem Cells Int 2017:3945403
59. Spyridopoulos I, Arthur HM (2017) Microvessels of the heart: formation, regeneration, and dysfunction. Microcirculation. 24:e12338
60. Zhang H, Zhu SJ, Wang W, Wei YJ, Hu SS (2008) Transplantation of microencapsulated genetically modified xenogeneic cells augments angiogenesis and improves heart function. Gene Ther 15:40–48
61. Behfar A, Crespo-Diaz R, Terzic A, Gersh BJ (2014) Cell therapy for cardiac repair—lessons from clinical trials. Nat Rev Cardiol 11:232–246
62. Behfar A, Terzic A (2006) Derivation of a cardiopoietic population from human mesenchymal stem cells yields cardiac progeny. Nat Clin Pract Cardiovasc Med 3(Suppl 1):S78–S82
63. Birchler A, Berger M, Jaggin V, Lopes T, Etzrodt M, Misun PM, Pena-Francesch M, Schroeder T, Hierlemann A, Frey O (2016) Seamless combination of fluorescence-activated cell sorting and hanging-drop networks for individual handling and culturing of stem cells and microtissue spheroids. Anal Chem 88:1222–1229
64. Declercq HA, De Caluwe T, Krysko O, Bachert C, Cornelissen MJ (2013) Bone grafts engineered from human adipose-derived stem cells in dynamic 3D-environments. Biomaterials 34:1004–1017
65. Dissanayaka WL, Zhu L, Hargreaves KM, Jin L, Zhang C (2014) Scaffold-free prevascularized microtissue spheroids for pulp regeneration. J Dent Res 93:1296–1303
66. Laschke MW, Schank TE, Scheuer C, Kleer S, Schuler S, Metzger W, Eglin D, Alini M, Menger MD (2013) Three-dimensional spheroids of adipose-derived mesenchymal stem cells are potent initiators of blood vessel formation in porous polyurethane scaffolds. Acta Biomater 9:6876–6884
67. Jakob W, Jentzsch KD, Mauersberger B, Heder G (1978) The chick embryo choriallantoic membrane as a bioassay for

angiogenesis factors: reactions induced by carrier materials. Exp Pathol 15:241–249
68. Ribatti D (2010) The chick embryo chorioallantoic membrane in the study of angiogenesis and metastasis concluding remarks. Springer, Dordrecht, pp 87–88
69. Spanelborowski K, Schnapper U, Heymer B (1988) The chick chorioallantoic membrane assay in the assessment of angiogenic factors. Biomed Res 9:253–260

Affiliations

Petra Wolint[1] · Annina Bopp[1,2] · Anna Woloszyk[1,2] · Yinghua Tian[1,3] · Olivera Evrova[1,4,5] · Monika Hilbe[6] · Pietro Giovanoli[1,5] · Maurizio Calcagni[1,5] · Simon P. Hoerstrup[2,7] · Johanna Buschmann[1,5] · Maximilian Y. Emmert[2,7,8]

[1] Division of Surgical Research, University Hospital of Zurich, Zurich, Switzerland

[2] Institute for Regenerative Medicine (IREM), University of Zurich, Zurich, Switzerland

[3] Visceral and Transplant Surgery, University Hospital Zurich, Zurich, Switzerland

[4] Laboratory of Applied Mechanobiology, ETH Zurich, Zurich, Switzerland

[5] Plastic Surgery and Hand Surgery, University Hospital Zurich, Zurich, Switzerland

[6] Institute of Veterinary Pathology, University of Zurich, Zurich, Switzerland

[7] Wyss Translational Center Zurich, University Zurich & ETH Zurich, Zurich, Switzerland

[8] University Heart Center, University Hospital Zurich, Rämistrasse 100, 8091 Zurich, Switzerland